

Supporting Information

Sub-ns Triplet State Formation by Non-Geminate Recombination in PSBTBT:PC₇₀BM and PCPDTBT:PC₆₀BM Organic Solar Cells

Fabian Etzold, Ian A. Howard, Nina Forler, Anton Melnyk, Denis Andrienko, Michael Ryan Hansen,* and Frédéric Laquai*

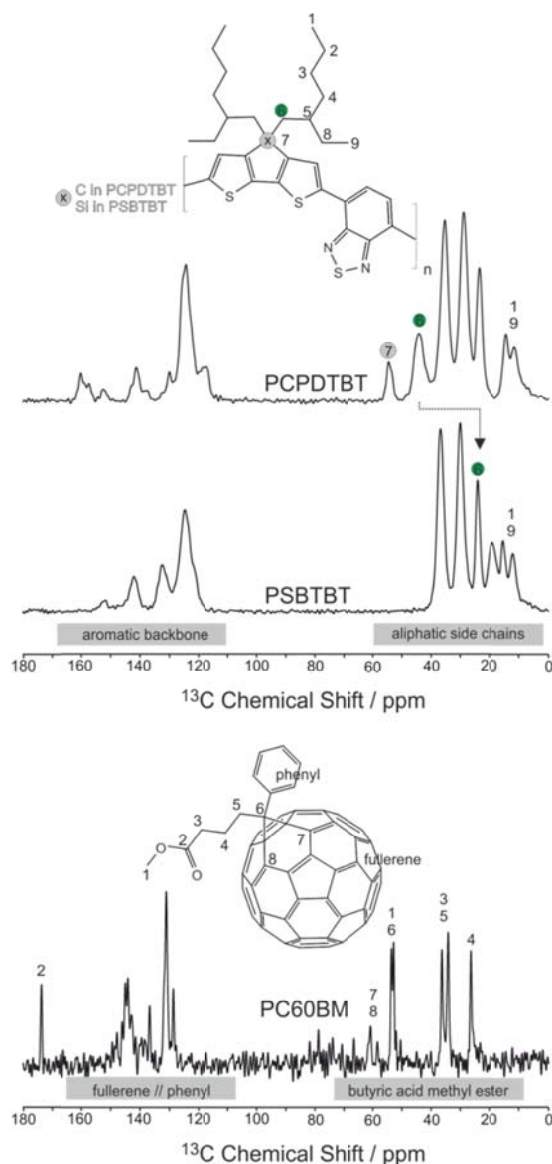


Figure S1: 1D $^{13}\text{C}\{^1\text{H}\}$ CP/MAS NMR spectra of PCPDTBT (top), PSBTBT (middle) and PC₆₀BM (bottom) together with their respective signal assignment. Highlighted in grey is the bridging carbon atom (C7) in PCPDTBT. The spectrum of PSBTBT is characterized by the absence of this resonance. The impact on the ^{13}C chemical shift for C6 due to silicon substitution is shown by an arrow and highlighted in green. In 2D $^{13}\text{C}\{^1\text{H}\}$ FSLG-HETCOR NMR, the absence of carbon atom C6 correlation signals reveals changes in angles and packing of the 2-ethylhexyl side chains upon addition of 2,44 % ODT to the solvent (see Figure 1).

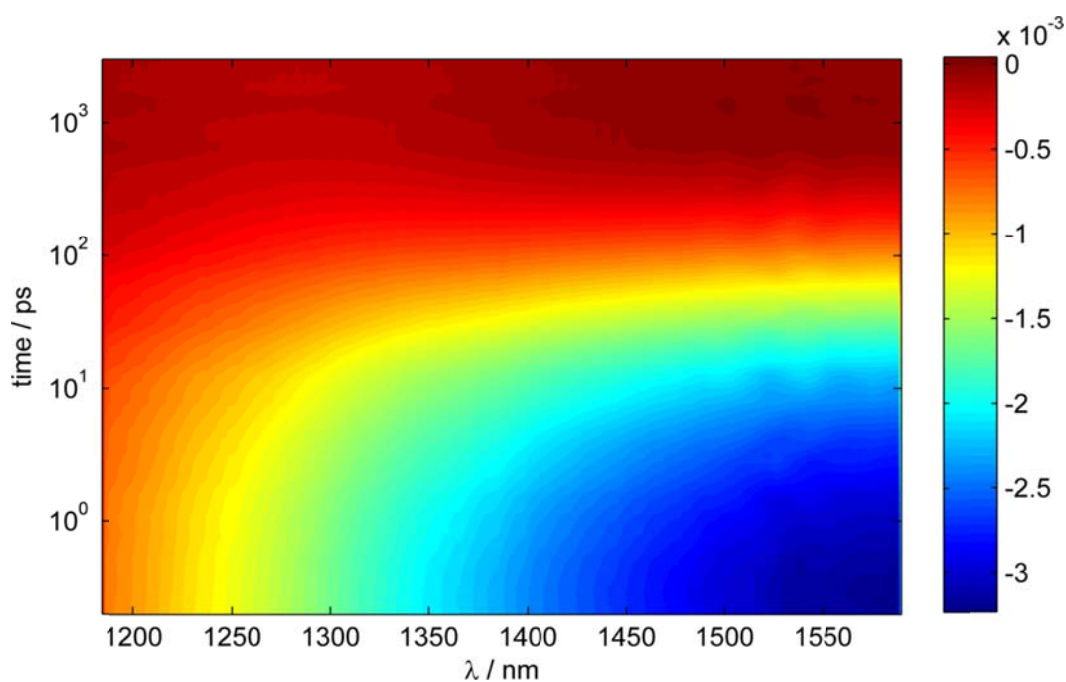


Figure S2: fs-ns $\Delta T/T$ data of pristine PSBTBT after excitation at 800nm with $1.5\mu\text{J}/\text{cm}^2$.

Factorization of TA data

In order to determine the number of excited states contributing to the TA data matrix, we performed an evolving factor analysis (EFA), starting right after the polymer singlet exciton quenching was completed. EFA is based on singular value decompositions (SVDs) performed on a sequence of sub-matrices, which are generated by successively increasing the number of columns contained in the sub-matrix considered for each decomposition.^[1] This procedure is repeatedly performed starting from the right side and from the left side of the data matrix. EFA yields information about the rank of the data matrix at each time point and thus it determines the number of relevant states that comprise the TA data matrix. EFA was performed on the PSBTBT:PC₇₀BM blend's sub-ns TA NIR data for five different excitation densities after excitation of the polymer at 800 nm. At approximately 10 ps, that is, the time required to ensure complete exciton quenching, all measurements are dominated by one excited state, namely component 1. However, a second component (2) is observed at later times whose onset shifts to earlier times with increasing pump fluence, indicating a fluence-dependent generation process (see also figure S3). The initial guess for the concentration profiles is then obtained by combining the forward and backward EFA.

The result of a transient absorption experiment is a two-dimensional data matrix containing the transient absorption spectra of each time point of the experiment. Assuming that the spectra of the individual excited states do not evolve or shift with time, the data matrix D can be written as a bilinear decomposition, in such a way that

$$D = CS + E.$$

C contains the concentration profiles of the excited states, the rows of S represent the transient absorption spectra of the states, and E ideally only contains experimental noise. In order to factorize the experimentally obtained data matrix and to determine the concentration profiles and cross-sections of the individual excited states, we employed multivariate curve resolution. Multivariate curve resolution is a soft-modeling approach used to analyze transient absorption data, independent of any a priori knowledge of the excited states that constitute the data matrix. Our analysis is based on the MCR-ALS algorithm developed by Tauler et al.,^[2] and a detailed discussion of the application of this technique to TA data has recently been presented by us.^[1] The inherent advantage of a soft-modeling method is its intrinsic independence from any photophysical model typically required for the data analysis. Compared to hard-modeling, in which a kinetic model of coupled rate equations is used on the basis of an a priori known number of excited and ground states and interconversion channels between them, neither any assumption of the number of excited states nor their decay processes is required to perform an MCR-ALS analysis. Instead, the number of excited states and the initial concentration profiles describing the transient data surface are determined in an evolving factor analysis (EFA) as shown in figure S4.

Subsequent matrix division yields the corresponding spectra, while constraints such as non-negativity of concentrations and non-positivity / non-negativity of the spectra can be applied. From the obtained spectra, a new set of concentration profiles is calculated and the procedure is repeated until a given tolerance criterion is met. However, the factorization of a data surface that is described by multiple species is never unique. Hence, an obtained solution is not necessarily a physically meaningful solution as can easily be seen from the following mathematical transformation:

$$D = CS = (CT)(T^{-1}S) = C_{new}S_{new}$$

In fact, any invertible matrix T generates a new set of concentration profiles, namely C_{new} , and spectra, namely S_{new} , equally-well describing the experimental data surface. We showed recently that in the case of two species with one known spectrum the rotational ambiguity can be expressed as a single parameter.^[1] This was used in the data analysis to quantify the uncertainty of our calculated solutions (see figure S5). Furthermore, we factorized the data measured at different pump fluences in one augmented data matrix, thereby guaranteeing that the calculated spectra are equal for all experimentally measured fluences.

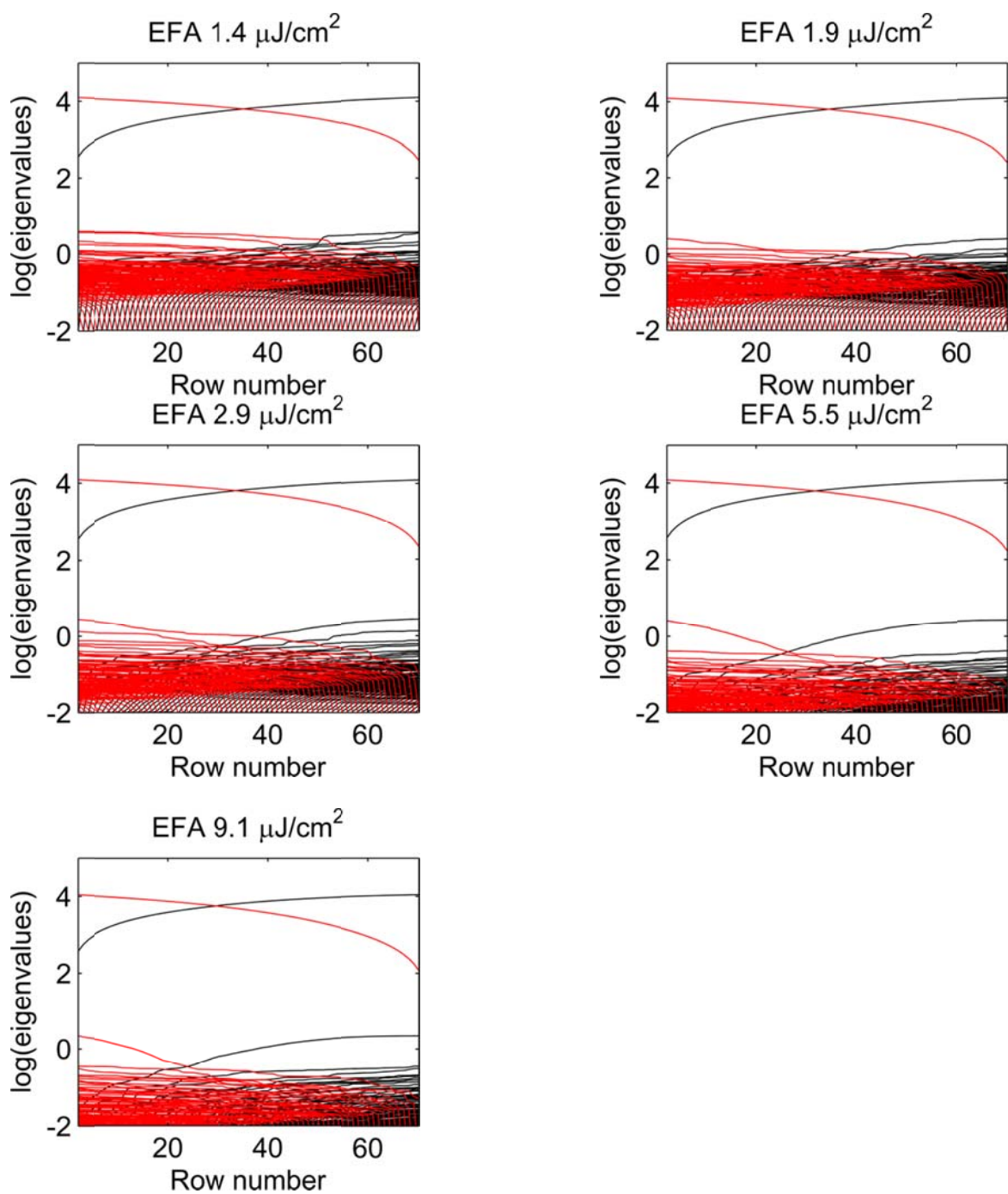


Figure S3: EFA of fs-ns TA data of PSBTBT:PC₇₀BM after excitation at 800nm for five different fluences. The black lines represent the forward, the red lines the backward EFA. The different row numbers indicate different time points. The EFA was started directly after exciton quenching (~10ps).

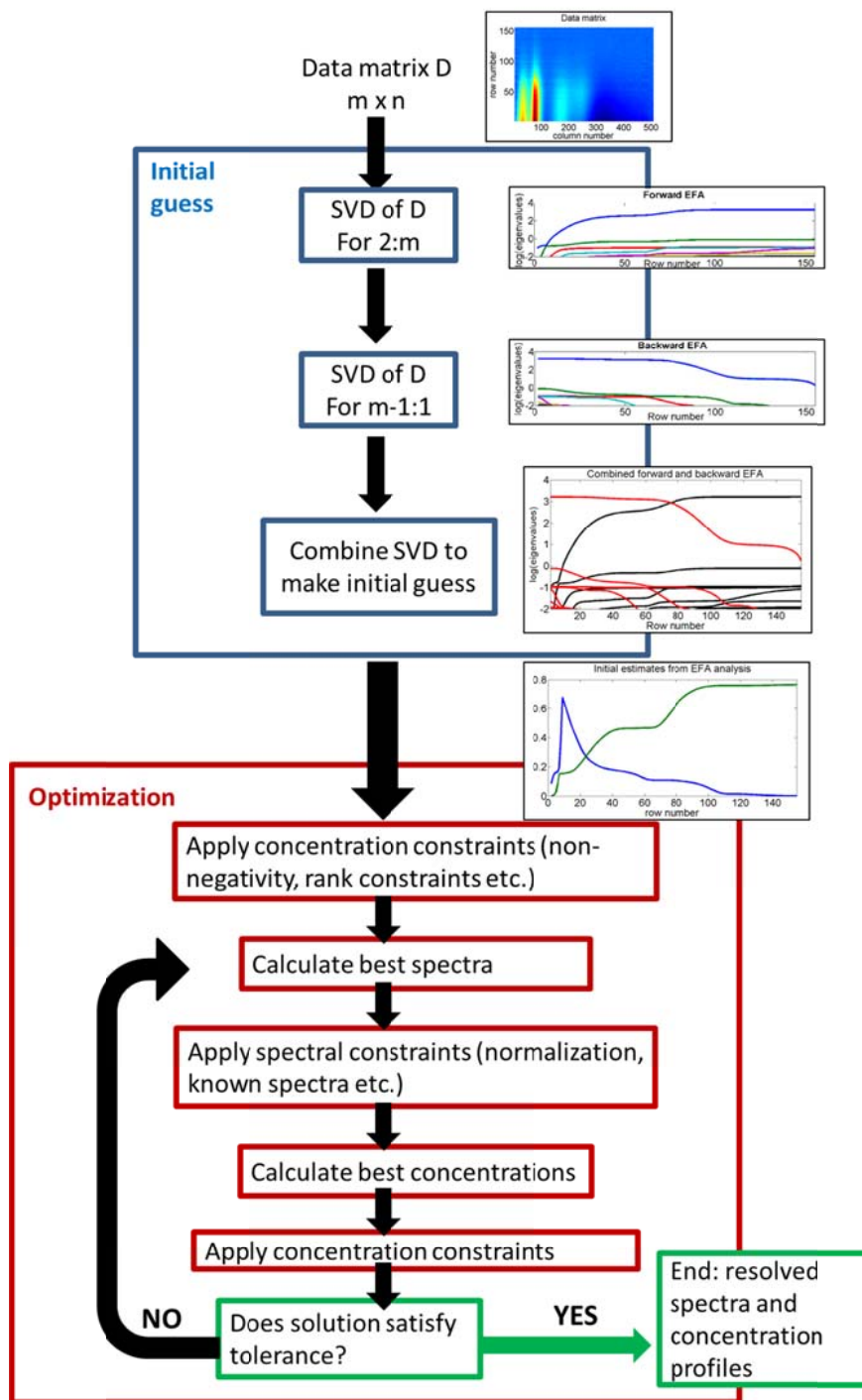


Figure S4: Flowchart of the MCR analysis with EFA as an initial guess.

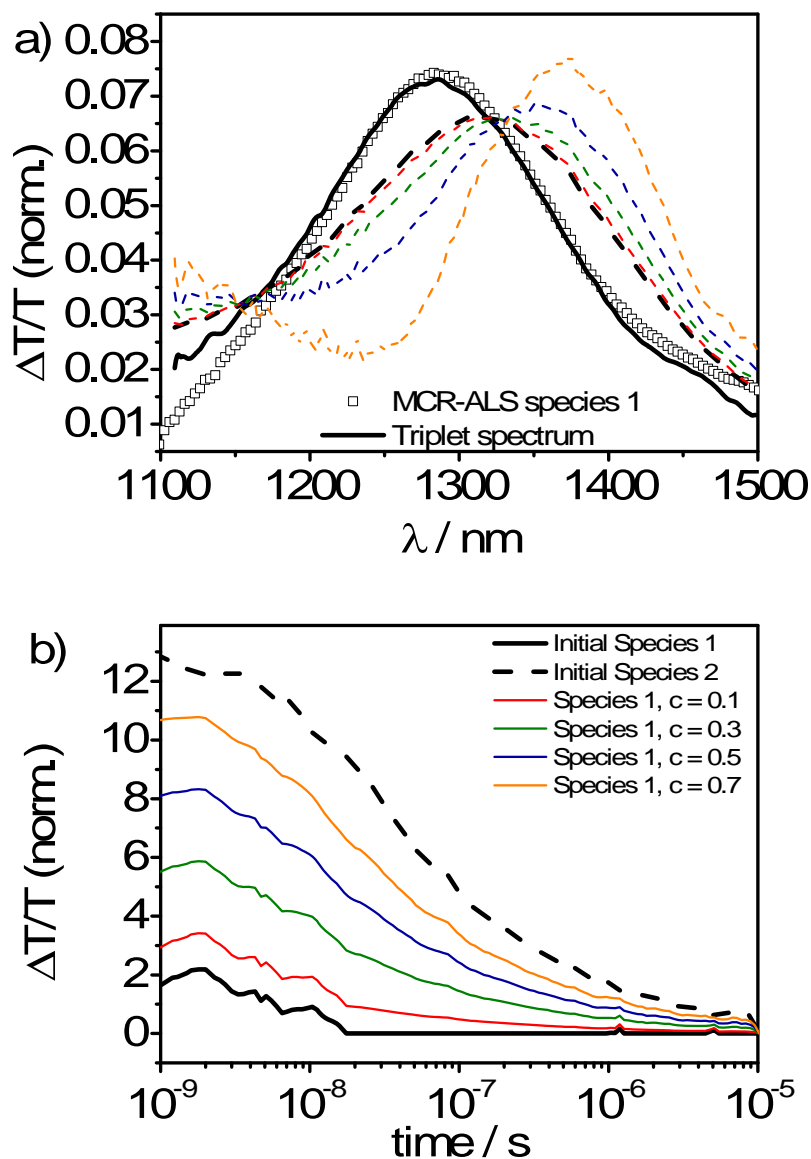


Figure S5: MCR-ALS analysis of PSBTBT:PC₇₀BM ns- μ s TA data. a) The open squares represent the spectrum of species 1 obtained from MCR-ALS and the black dashed line is spectrum 2 obtained from MCR-ALS. The solid black line is the triplet spectrum measured on a PSBTBT:PtOEP blend. The colored dashed lines represent rotations of species 2 for species 1 being fixed to the triplet spectrum. b) Corresponding concentration profiles. Note that for the rotations only the concentration profiles of species 1 are displayed, as rotation of species 2 with a fixed spectrum of species 1 only scales the concentration profiles of species 2.

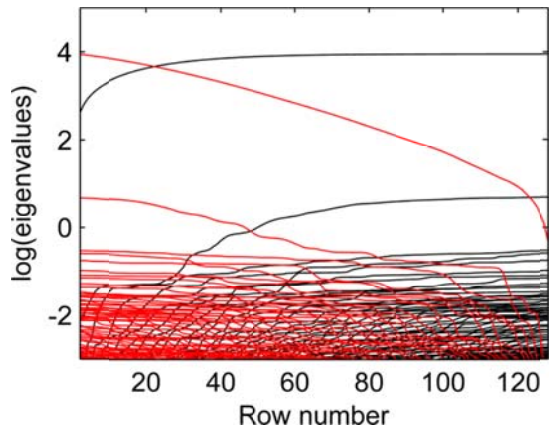


Figure S6: EFA of long time PSBTBT:PC₇₀BM data excited at 532nm with 2.9 μ J/cm². The black lines represent the forward EFA, the red lines are the backward EFA.

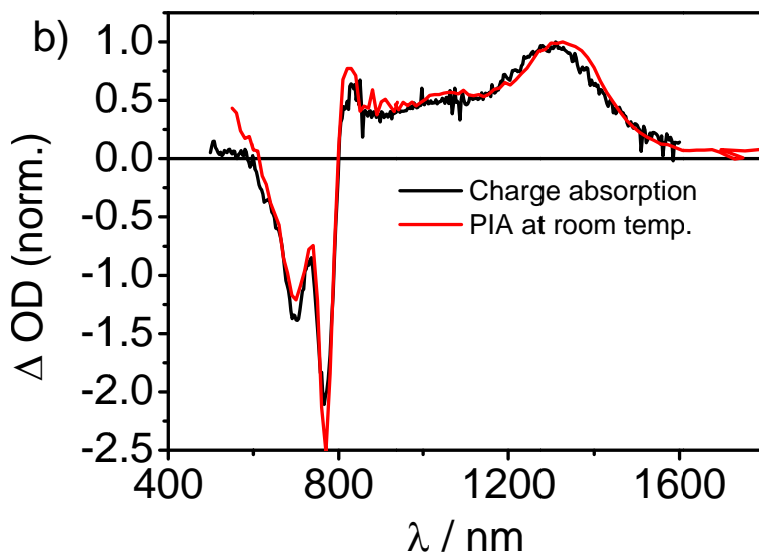
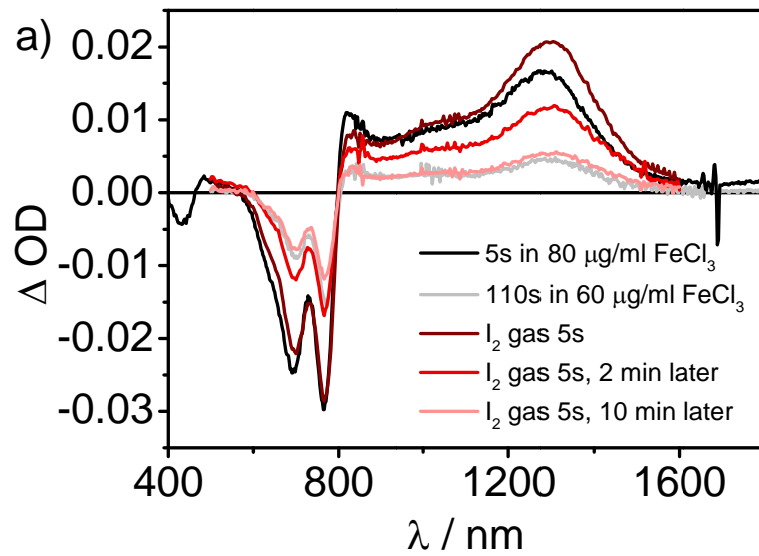


Figure S7: Oxidation experiments performed on PSBTBT:PC₇₀BM. a) Differential absorption spectra after oxidation by FeCl₃ in acetonitrile and iodine vapor. For oxidation with FeCl₃ the blend films were dipped into the FeCl₃ solution and rinsed with acetonitrile to get rid of additional FeCl₃. For oxidation in iodine vapor, the blend films were placed in iodine gas and subsequently measured for several times as the oxidation appeared to be reversible with iodine. b) Comparison of the charge absorption obtained from oxidation with the cw-PIA spectrum of the blend.

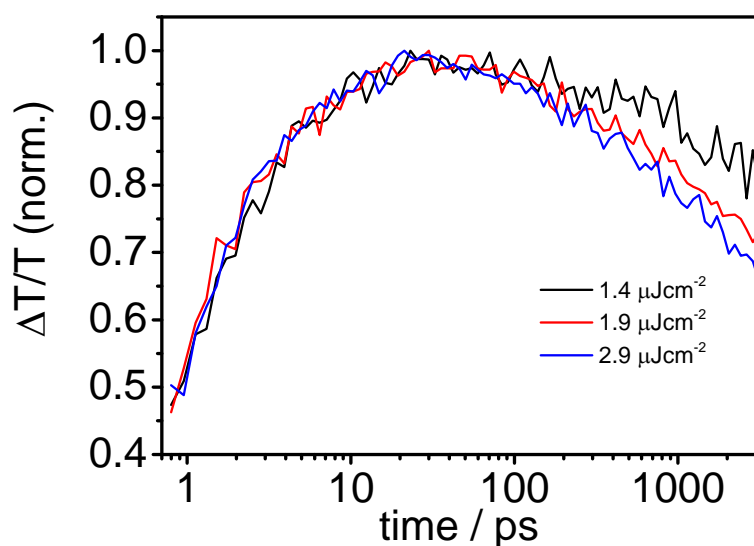
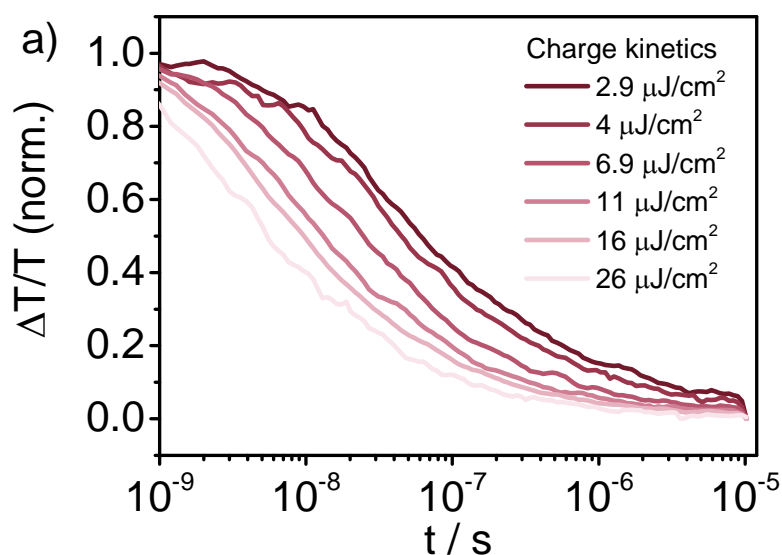


Figure S8: Normalized charge kinetics in PSBTBT:PC₇₀BM.



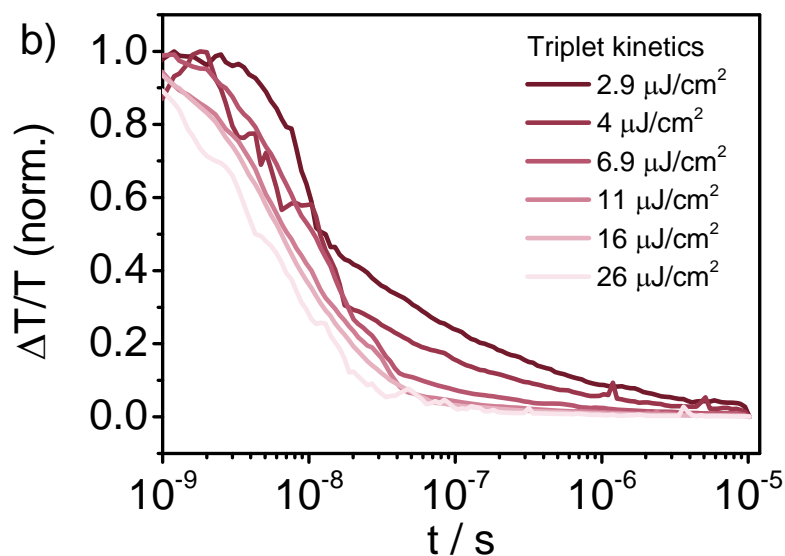


Figure S9: Normalized concentration profiles of the charges (a) and triplets (b) for different excitation fluences in PSBTBT:PC₇₀BM.

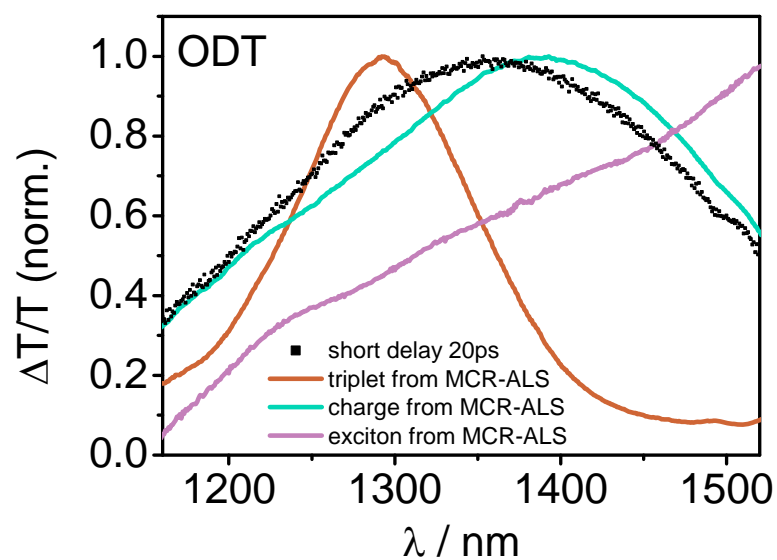


Figure S10: MCR-ALS results of the ns- μs TA data of PCPDTBT:PC₆₀BM prepared with ODT. The exciton spectrum is obtained from measurements on pristine PCPDTBT. The squares represent the short time TA spectrum of the blend after 20ps delay.

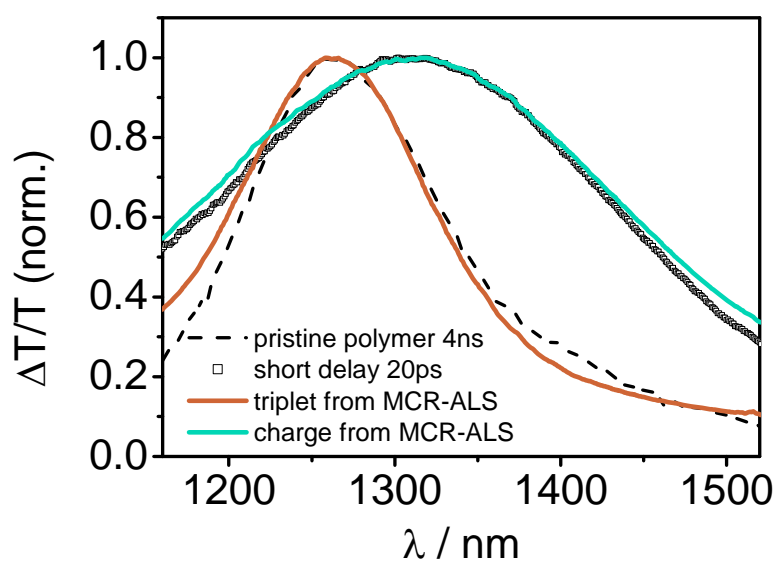
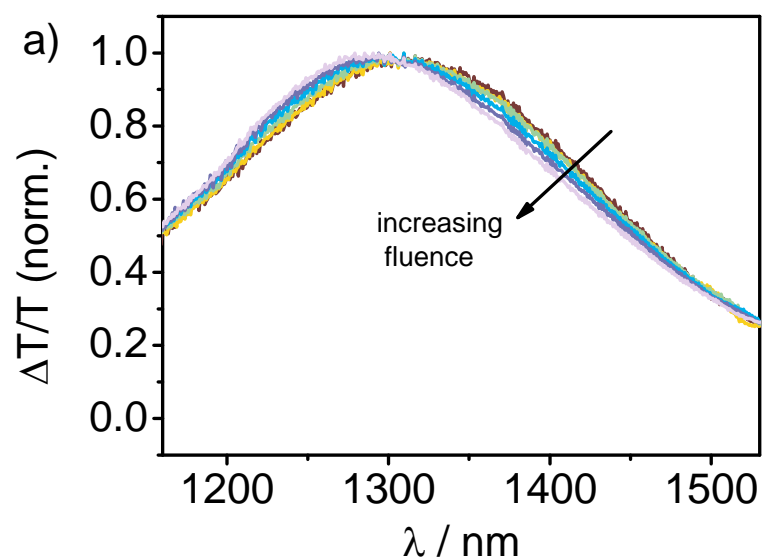


Figure S11: MCR-ALS results of the ns- μ s TA data of PCPDTBT:PC₆₀BM prepared without ODT. The squares represent the short time TA spectrum of the blend after 20ps delay, and the dashed line is the triplet spectrum obtained from measurements on the pristine material.



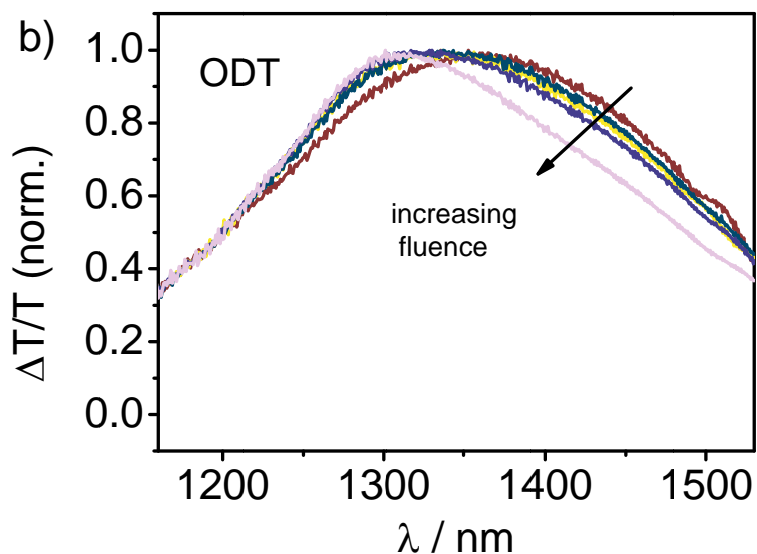


Figure S12: TA spectra after 20ps delay of PCPDTBT:PC₆₀BM prepared without (a) and with ODT (b) obtained after excitation with 800nm for different fluences.

Residuals of the factorization

The residuals of the MCR-ALS analysis are calculated by taking the difference between the simulated data matrix and the experimental data matrix. The data matrix contains the $\Delta T/T$ values of all fluences stacked along the y-axis, where each fluence is normalized to its maximum.

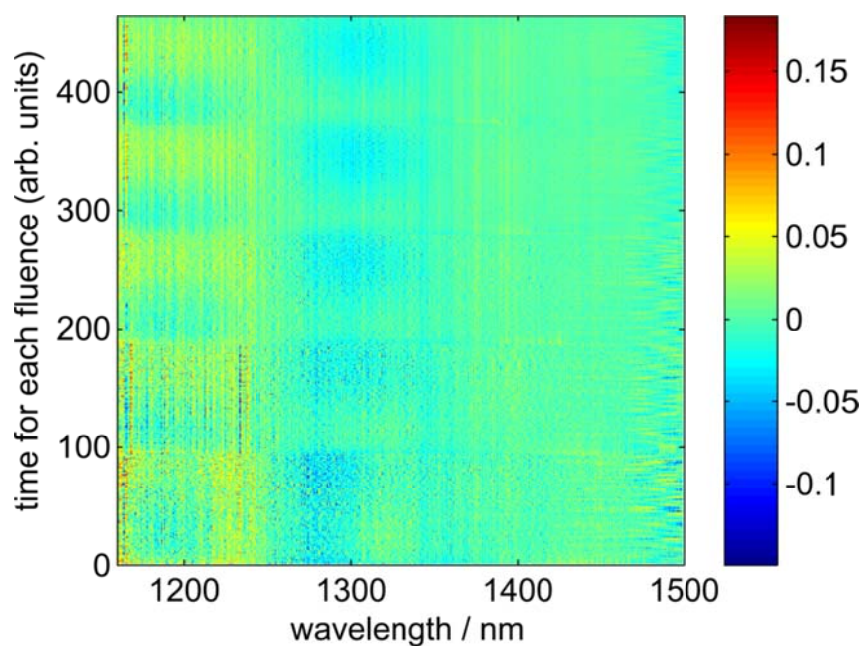


Figure S13: Error of the factorization of the fs-ns TA data of PSBTBT:PC₇₀BM after excitation at 800nm.

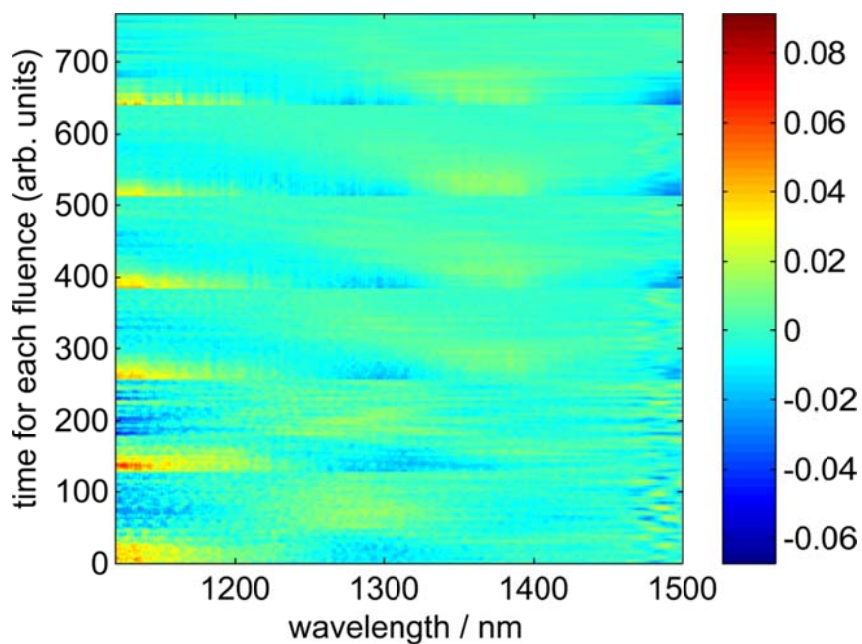


Figure S14: Error of the factorization of the ns- μ s TA data of PSBTBT:PC₇₀BM after excitation at 532nm.

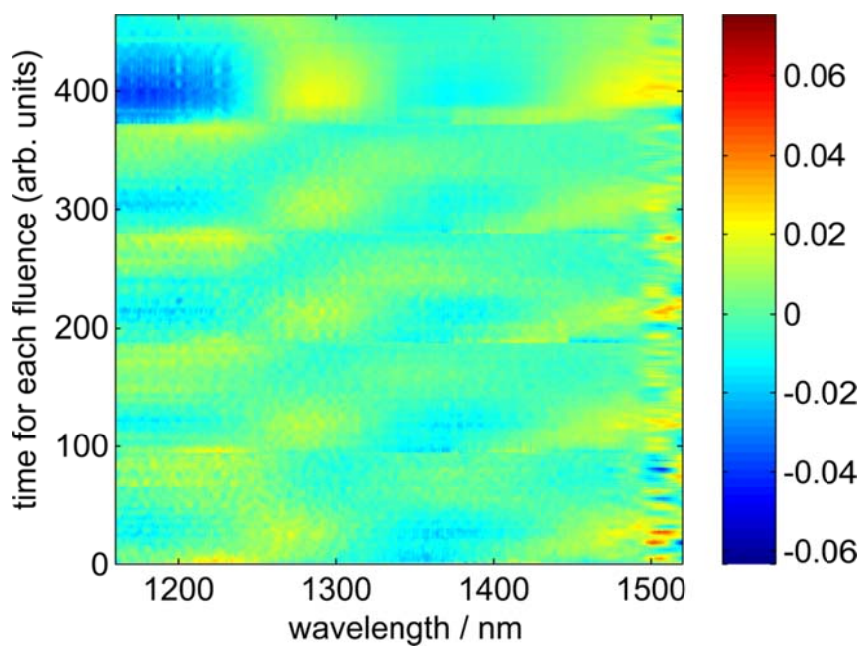


Figure S15: Error of the factorization of the fs-ns TA data of PCPDTBT:PC₆₀BM prepared with ODT after excitation at 800nm.

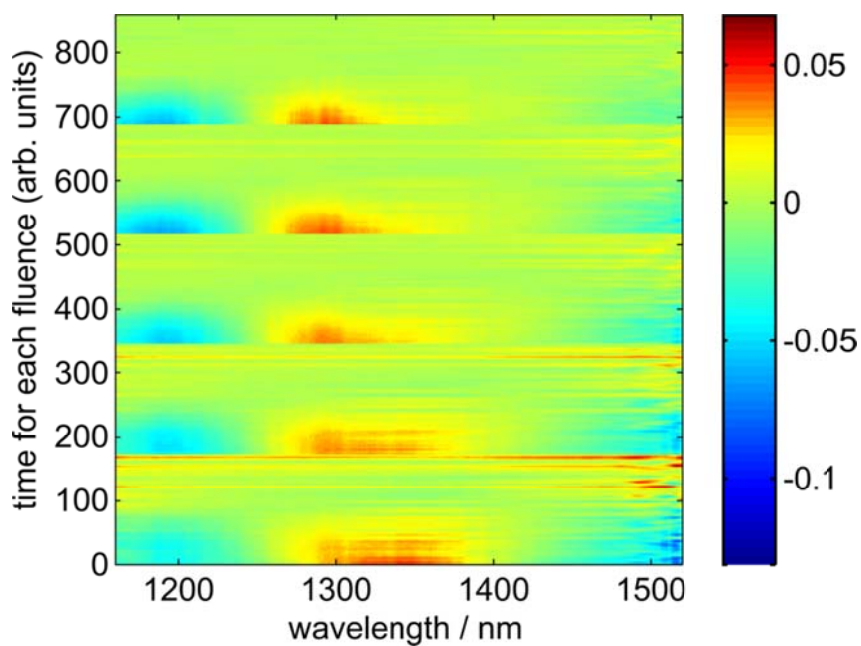


Figure S16: Error of the factorization of the ns- μ s TA data of PCPDTBT:PC₆₀BM prepared with ODT after excitation at 532nm.

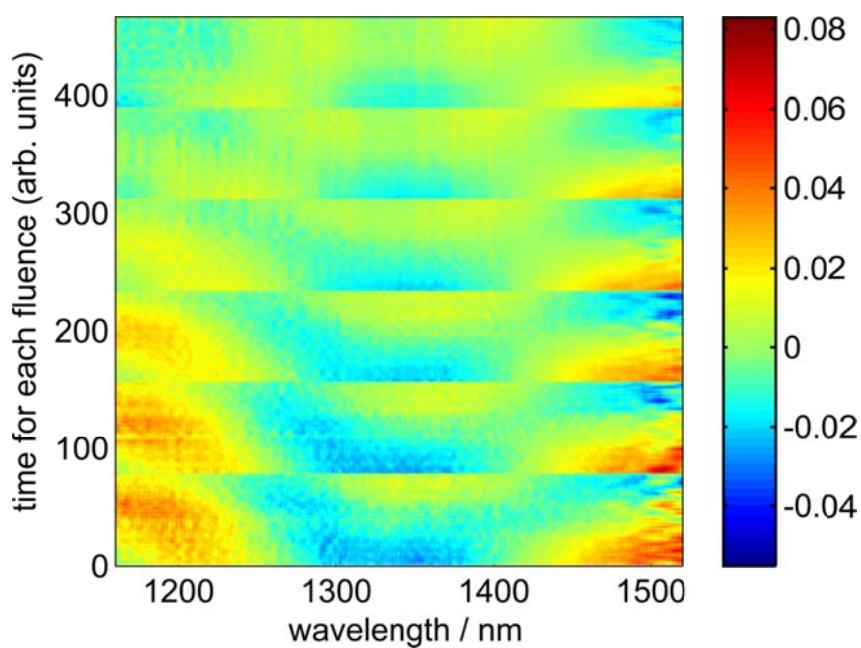


Figure S17: Error of the factorization of fs-ns TA data of PCPDTBT:PC₆₀BM prepared without ODT after excitation at 800nm.

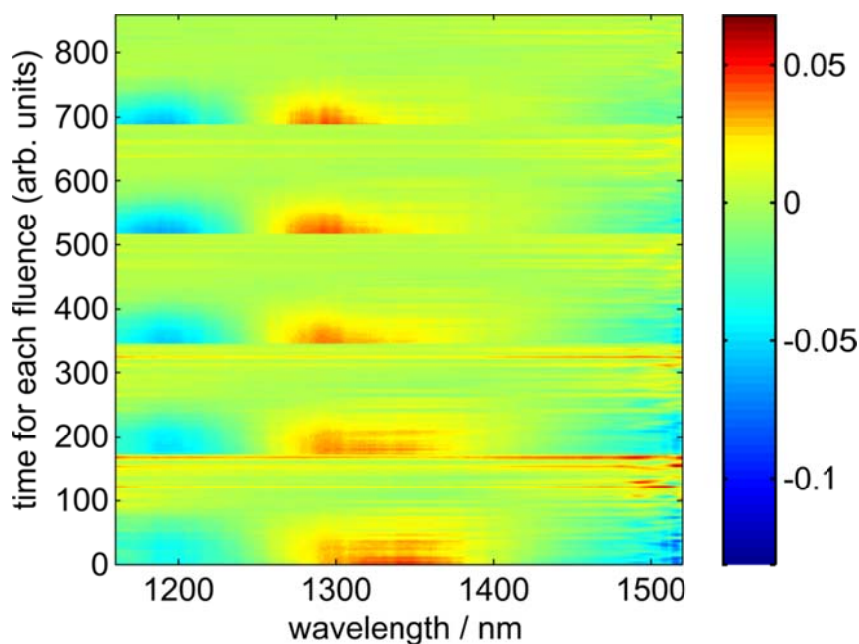


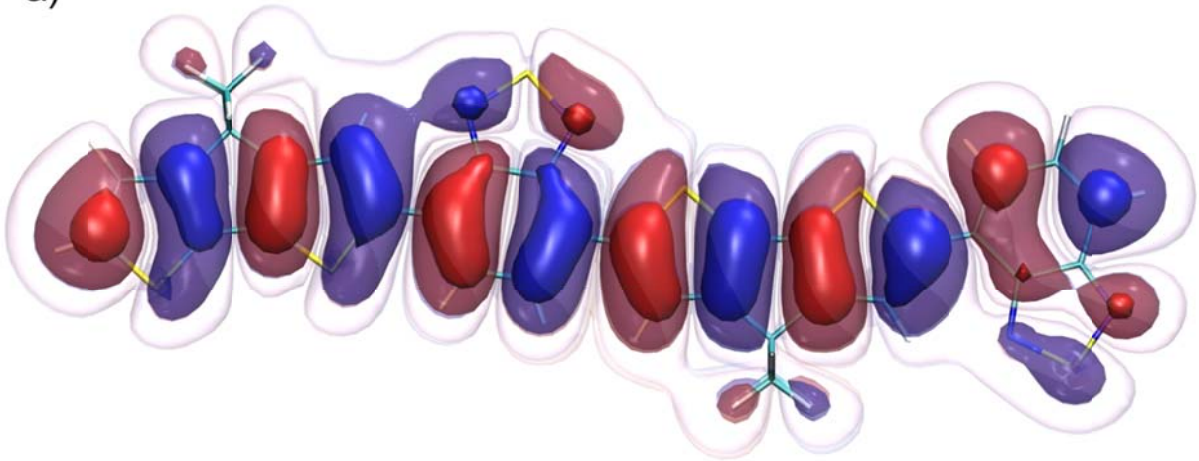
Figure S18: Error of the factorization of the ns- μ s TA data of PCPDTBT:PC₆₀BM prepared without ODT after excitation at 532nm.

First principles calculations

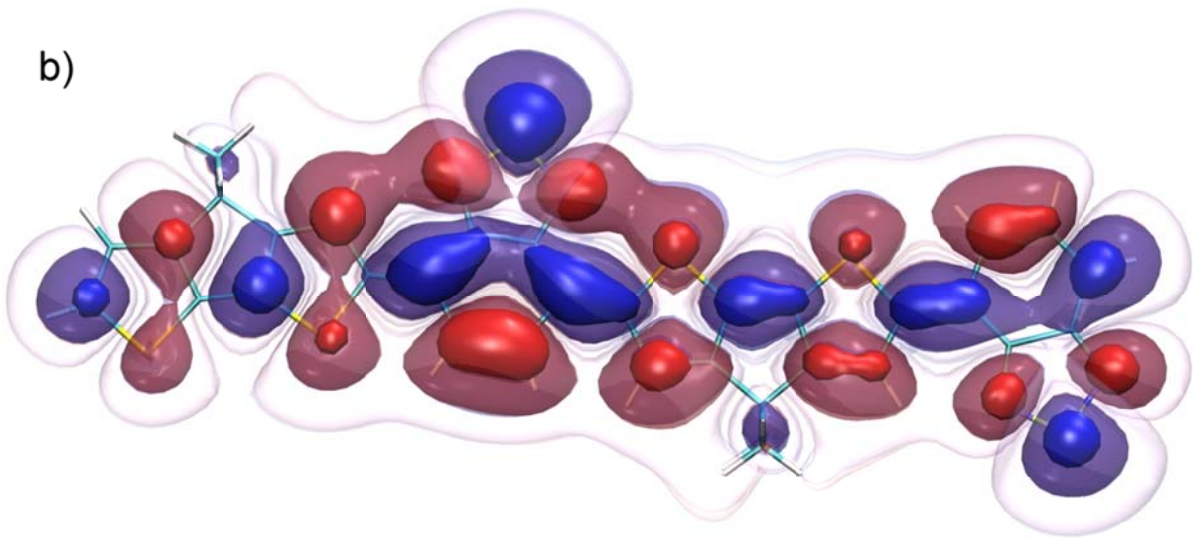
All calculations were performed at B3LYP/6-311g(d,p) level of theory using the Gaussian 09 program.^[3] Excited states were computed using time dependent density functional theory. Oligomers up to a tetramer were studied, where the tetramer corresponds to the localization of Frenkel excitons.^[4]

HOMO/LUMO orbitals, which are shown in Fig. S12, have no significant differences, which is also supported by similar energy levels of these two polymers, shown in Fig S19 (a). The excited state energies are slightly higher in case of PSBTBT, however the offset between triplet and singlet levels is practically the same.

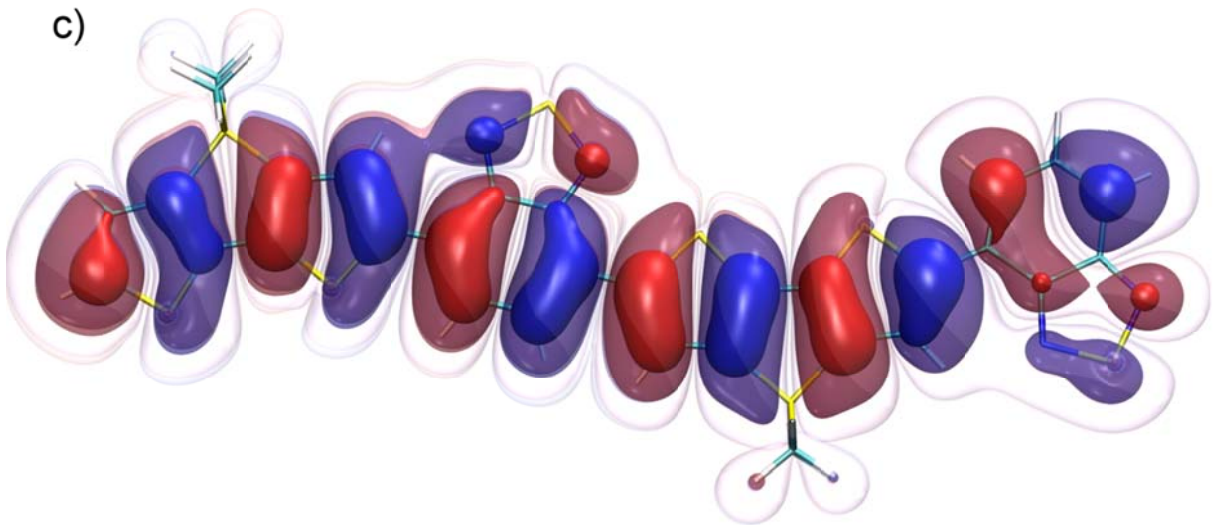
a)



b)



c)



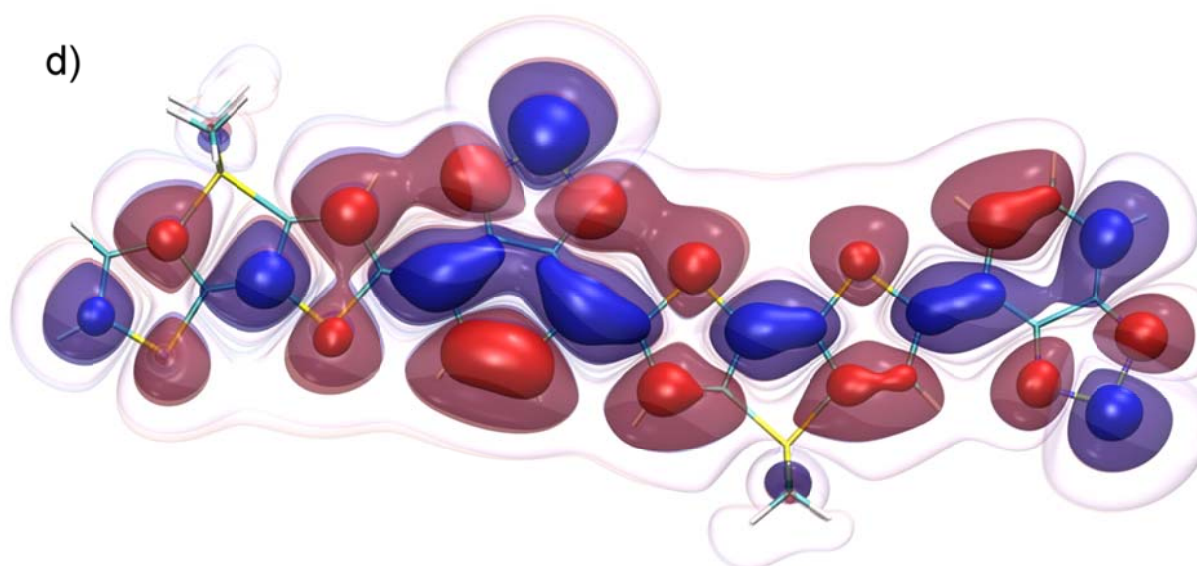
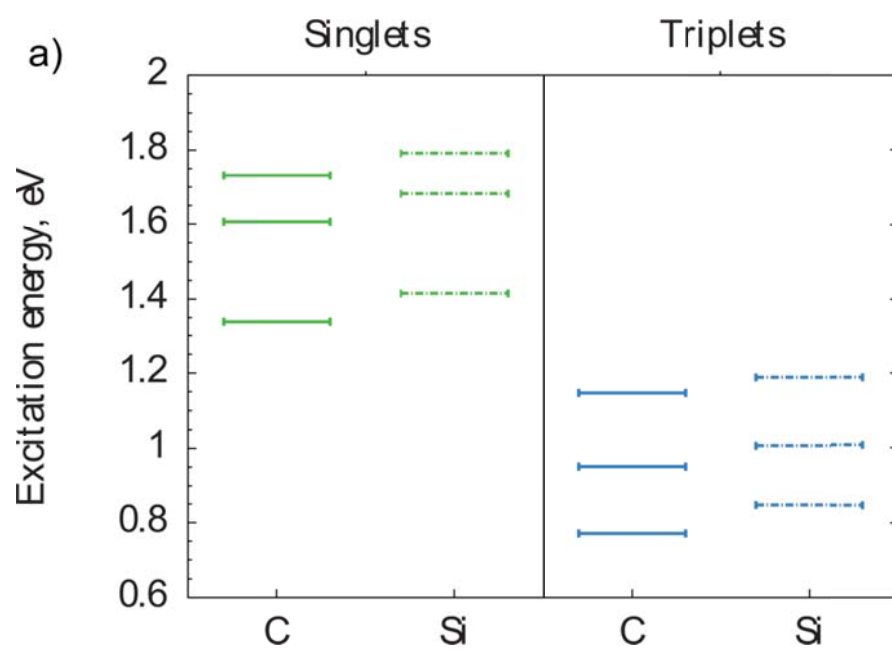


Figure S19: HOMO and LUMO orbitals of (a,b) PCPDTBT and (c,d) PSBTBT.



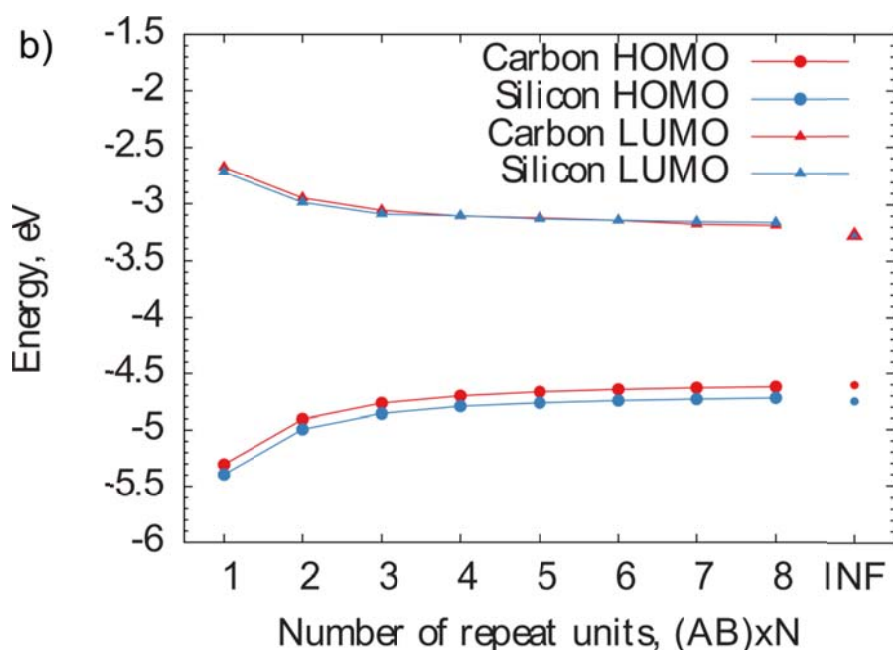


Figure.S20: (a) HOMO/LUMO levels as a function of oligomer length and (b) excited state energies of a tetramer of PCPDTBT and PSBTBT.

- [1] I. A. Howard, H. Mangold, F. Etzold, D. Gehrig, F. Laquai, in *Ultrafast Dynamics in Molecules, Nanostructures and Interfaces*, World scientific, 2013.
- [2] a) A. de Juan, R. Tauler, *Anal. Chim. Acta* **2003**, *500*, 195; b) A. de Juan, M. Maeder, M. Martínez, R. Tauler, *Chemom. Intell. Lab. Syst.* **2000**, *54*, 123; c) J. Jaumot, R. Gargallo, A. de Juan, R. Tauler, *Chemom. Intell. Lab. Syst.* **2005**, *76*, 101; d) A. de Juan, R. Tauler, *Crit. Rev. Anal. Chem.* **2006**, *36*, 163.
- [3] M. J. Frisch, G. W. Trucks, H. B. Schlegel, G. E. Scuseria, M. A. Robb, J. R. Cheeseman, G. Scalmani, V. Barone, B. Mennucci, G. A. Petersson, H. Nakatsuji, M. Caricato, X. Li, H. P. Hratchian, A. F. Izmaylov, J. Bloino, G. Zheng, J. L. Sonnenberg, M. Hada, M. Ehara, K. Toyota, R. Fukuda, J. Hasegawa, M. Ishida, T. Nakajima, Y. Honda, O. Kitao, H. Nakai, T. Vreven, J. A. Montgomery Jr., J. E. Peralta, F. Ogliaro, M. J. Bearpark, J. Heyd, E. N. Brothers, K. N. Kudin, V. N. Staroverov, R. Kobayashi, J. Normand, K. Raghavachari, A. P. Rendell, J. C. Burant, S. S. Iyengar, J. Tomasi, M. Cossi, N. Rega, N. J. Millam, M. Klene, J. E. Knox, J. B. Cross, V. Bakken, C. Adamo, J. Jaramillo, R. Gomperts, R. E. Stratmann, O. Yazyev, A. J. Austin, R. Cammi, C. Pomelli, J. W. Ochterski, R. L. Martin, K. Morokuma, V. G. Zakrzewski, G. A. Voth, P. Salvador, J. J. Dannenberg, S. Dapprich, A. D. Daniels, Ö. Farkas, J. B. Foresman, J. V. Ortiz, J. Cioslowski, D. J. Fox, Gaussian, Inc., Wallingford, CT, USA 2009.
- [4] B. Baumeier, M. Rohlfing, D. Andrienko, *J. Chem. Theory Comput.* **2014**, *10*, 3104.